Improved NbN Phonon Cooled Hot Electron Bolometer Mixers

M.Hajenius[1,2], J.J.A. Baselmans[2], J.R. Gao[1,2], T.M. Klapwijk[1], P.A.J. de Korte[2], B. Voronov[3] and G. Gol'tsman[3]

[1]Department of Nanoscience, Delft University of Technology, Lorentzweg 1, 2628 CJ Delft, The Netherlands.

[2]Space Research Organisation Netherlands, Sorbonnelaan 2, 3584 CA Utrecht, The Netherlands

[3]Moscow State Pedagogical University, Moscow 119435, Russia.

Abstract

NbN phonon-cooled hot electron bolometer mixers (HEBs) have been realized with negligible contact resistance to Au pads. By adding either a 5 nm Nb or a 10 nm NbTiN layer between the Au and NbN, to preserve superconductivity in the NbN under the Au contact pad, superior noise temperatures have been obtained. Using DC I,V curves and resistive transitions in combination with process parameters we analyze the nature of these improved devices and determine interface transparencies.

1. Introduction

Currently, for frequencies beyond 1 THz, superconducting hot electron bolometers (HEB's) appear to be the only option for low noise heterodyne mixing elements. Phonon-cooled HEB's, based on thin superconducting NbN with a fast electron-phonon cooling time, are particularly promising because they combine a high sensitivity with a reasonably large intermediate frequency (IF) roll-off [1-6]. However, these detectors have not yet reached the ultimate sensitivity limit set by quantum noise: $\hbar\omega / k_b$, in which $\hbar$ is Plank's constant, ω the angular frequency, and k_b is Boltzman's constant. Further progress, both theoretically and experimentally, is critically dependent on a proper understanding of the device-operation. Originally it was proposed that these devices would exploit the strong temperature dependence of the resistive transition. However, it has become clear that both diffusion-cooled and phonon-cooled devices are based on an electronic hot spot, formed because they are biased with a relatively high DC current. This resistive electronic hot spot of variable length has been identified as the source of the mixing process.

In a HEB the active superconducting material is in direct contact with an antenna structure, which also serves as electrodes for the dc bias. To minimize losses at the high frequencies a high conductivity normal metal, such as gold, is used. In a series of experiments we have recently learnt that improved mixing-performance can be realized by focusing on improved contacts between the NbN, optimized for phonon-cooling, and the Au electrodes. If an intermediate layer of Nb or NbTiN is inserted between the active NbN and the Au significantly better noise temperatures are reached. To date best receiver noise temperatures of *1000 K @ 2.5 THz* have been obtained with a device with a NbTiN intermediate layer. Details of the RF measurements can be found elsewhere [8].

In this paper we describe the various contacts we have developed and studied based on the DC I,V curves and resistive transitions. To understand the critical temperature of the different multi-layers appearing in the different contact structures we use a proximity-effect model for bi-layers [9].

2. Devices with different contacts

The NbN HEBs are based on a 3.5 nm thick NbN film on a Si substrate, produced at Moscow State Pedagogical University. These films, optimized for phonon-cooling, have a sheet resistance of 635 Ω, measured at 300 K, and after subsequent fabrication steps a T_c of ~ 9.9 K. The layout of a mixer together with a cross section of the contact structure is shown in Fig. 1. A spiral antenna of 120 nm thick Au (layer 1 in Fig. 1) is used to couple the RF and DC signal into the superconducting bridge. The connection between the bolometer itself (3) and the antenna is made by the contact structure, consisting of a gold layer ("2") and an intermediate layer ("4") on top of the NbN film. The intermediate layer consists of either a normal metal (Ti) as an adhesion layer or a superconductor (Nb or NbTiN). The latter is to avoid a proximity-effect induced destruction of the superconductivity in the NbN under the Au. Typical dimensions of the bridge are 4 μm in wide and 0.4 μm in length, measured between the contact-pads, the part of the NbN uncovered by any contact layer.

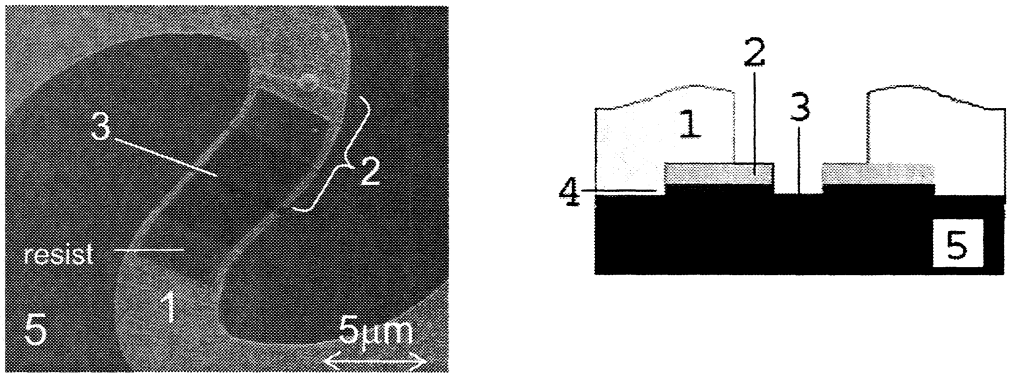

Figure 1. Spiral antenna coupled NbN HEB devices. On the left a SEM picture of the top view of a device and on the right a cross section of the device. "1" indicates the Au spiral antenna structure which is ~ 150 nm thick; "2" the Au layer on the contact pads; "3" the superconducting NbN film, which extends underneath the contact layer/antenna; "4" the intermediate layer between the Au and the NbN film; "5" the Si substrate.

The thin optimized NbN films have to become part of the antenna-structure. It was found [10] that they suffer from irreproducible contact resistances due to a native oxide or other surface contaminants on the NbN film. A short Ar^+ physical etching step is applied to remove such a contamination layer. To find an optimal recipe for the best contacts various experiments have been executed using the more readily available NbTiN layers. Fig. 2 shows the results of an Ar^+ etch calibration curve using a freshly made NbTiN thin film. The devices have been artificially contaminated by applying an O_2 plasma for 15 sec. Fig. 2 clearly shows, that an Ar^+ etch during more than 10 sec helps to reduce the contact resistance. These data are not yet conclusive because we could not deposit the subsequent the Ti/Au layer in the same vacuum system, where the Ar sputter etch is performed. Hence, the remaining resistance could be due to the brief exposure of the freshly cleaned film to ambient pressure. We should also point out that applied to a NbN film an Ar etch of 5 seconds already leads to a reduction of T_c by 0.5 K.

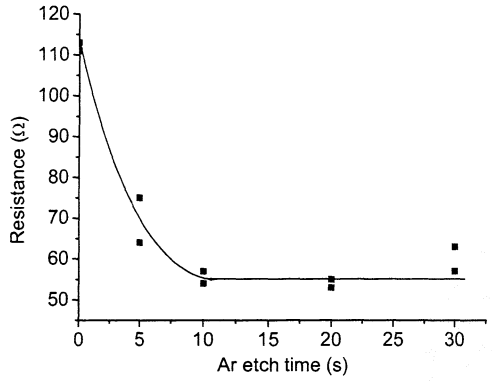

Fig. 2. Resistance of a HEB-like devices measured at a temperature above T_c plotted as a function of Ar^+ etch duration. Before Ar^- etching, the NbTiN has been artificially contaminated by an O_2 plasma for 15 sec. We note that for a plain NbN film, the effect of 5 s Ar^- etching is a decrease in T_c of ~ 0.5 K.

Minimizing a contact resistance between Au and NbN is attractive to reduce the losses and to avoid a voltage-drop in the device at a point where it cannot be an active part of the mixing process. However, a reduced contact resistance between the thick Au and the thin NbN means also an enhanced transparency for electronic exchange, or a maximally effective proximity-effect, which will lead to a destruction of the superconductivity in the NbN underneath the Au. To make sure that the uncovered NbN (Fig.1) would be the weakest link we also developed devices with a superconducting film inserted between the NbN and the Au to maintain superconductivity in the covered NbN.

We developed and studied four different types of contact structures. For clarity we first define our terminology. We will use the term *contact layer* for the composite layer of Au ("2") and the intermediate layer ("4") in Fig. 1, which is deposited on top of the NbN. We will use the term *contact pad* for the triple-stack layer of the NbN and the contact layer("4"+"2"). This triple-stack sets the boundary conditions for the signal fed to the active NbN layer and also for hot-spot formation. All device geometries are identical except for the contact layer and the treatment of the NbN surface prior to the deposition of the intermediate layer. All devices are made on a single wafer. Details of the four different types of contacts are listed below:

Type A: The contact layer is 5 nm Ti layer, introduced to improve Au adhesion, and *70 nm thick Au* on top. The interface to NbN is cleaned by a low power and low pressure O_2 plasma for 6 seconds, meant to remove resist-residues. The contact-layer ("4"+"2") is evaporated *ex situ* afterwards.

Type D: The contact layer is 5 nm Ti and *70 nm Au*. The interface to the NbN is prepared by cleaning first the residual e-beam resist using the same O_2 plasma cleaning as type A. Then an Ar^- physical etch cleaning (15 seconds) is performed. The metals are evaporated *ex-situ* afterwards.

Type H: The contact layer is *5 nm Nb* and *45 nm Au* on top. The interface to the NbN is made by cleaning first the residual e-beam resist using the same O_2 plasma, followed by an Ar^+ physical etch cleaning (15 seconds). The metals (of layers "4"+"2") are sputtered *in-situ* afterwards. Although we did not monitor the T_c of this Nb layer, from experience we expect it to be superconducting at a T_c of about 6 K.

Type G: The contact layer is *10 nm NbTiN* and *40 nm Au* on top. The interface to the NbN is prepared identically to the method used for type H. From previous measurements, we expect the intrinsic T_c of the NbTiN layer to be ~ 8 K.

Note that the O_2 plasma cleaning step is critical. If the duration is too short, not all residual e-beam resist is removed. But if too long, the O_2 plasma starts to oxidize the surface of the NbN [11]. To illustrate this point we present resistance versus temperature measurements (Fig.3) from a testbatch of HEB like devices using NbTiN as the active film. All devices have the same bridge dimensions, but with different O_2 plasma etch duration for the contacts. Starting with 4 seconds the device resistance first decreases, which we attribute to resist-residue removal. For etch times longer than 6 seconds the device resistance increases and the T_c drops. This combination of observations indicates a deterioration of the NbTiN film. We have subsequently used 6 sec as a value for optimized O_2 cleaning.

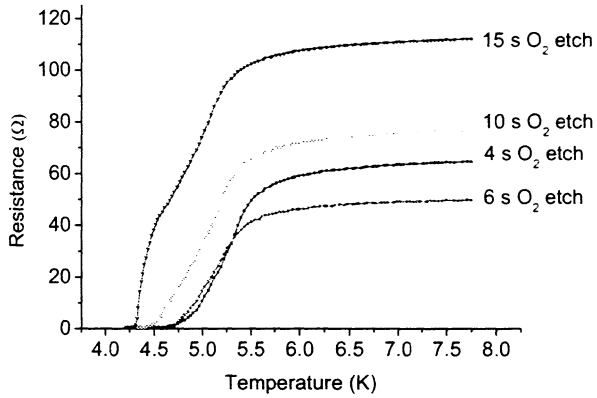

Fig.3. Resistance versus temperature measurements of HEB-like devices with various O_2 plasma cleaning duration before the metal contact pad is evaporated (ex-situ). In this case, a thin 4.5 nm NbTiN film with a lower T_c than the NbN is used. A clear reduction in T_c is observed for O_2 plasma etch durations longer than 10 s as well as an increase in resistance.

3. Resistance versus Temperature Measurements

We first compare the R(T) curves of type A and type D devices, which only differ with respect to interface cleaning (Fig. 4). In the normal state type A devices show a resistance of 170 Ω, which cannot be accounted for by the bridge resistance alone, using the known resistivity of the film. (Similar anomalously high resistance values for HEB's were reported before [10]). The resistance of type D devices is ~ 80 Ω and approaches the expected resistance of the bridge. Because the devices are identical except for the cleaning of the NbN film we associate the additional 120 Ω with the contact resistance between the active NbN bolometer and the contact layer. Obviously, the physical interface cleaning reduces the contact resistance significantly.

Upon cooling the devices we find that type A devices have only one superconducting transition temperature around 9.3 K. The type D devices show two transitions, one at 7 K (T_{c2}) and one at 9.9 K (T_{c1}). Since the measurements are two-point measurements on an effectively NSN one would not expect a full zero-voltage state. However, the resistive contribution of the Au is negligible on the scale of Fig.4 and all resistance must be due to the highly resistive NbN (apart from the contribution due to the interface). The lower transition

temperature T_{c2} observed for type D devices is attributed to the NbN underneath the contact layer. The highest transition temperature T_{c1} is assumed to be due to the bridge itself. The lower value of T_{c2} may be partly due to 15 sec Ar^+ etching and partly due to the superconducting proximity effect. Although not analyzed in detail it is reasonable to assume that the resistance "tail" between 7 and 9.5 K is due to the conversion of quasi-particle current to supercurrent and the associated resistance [14,15].

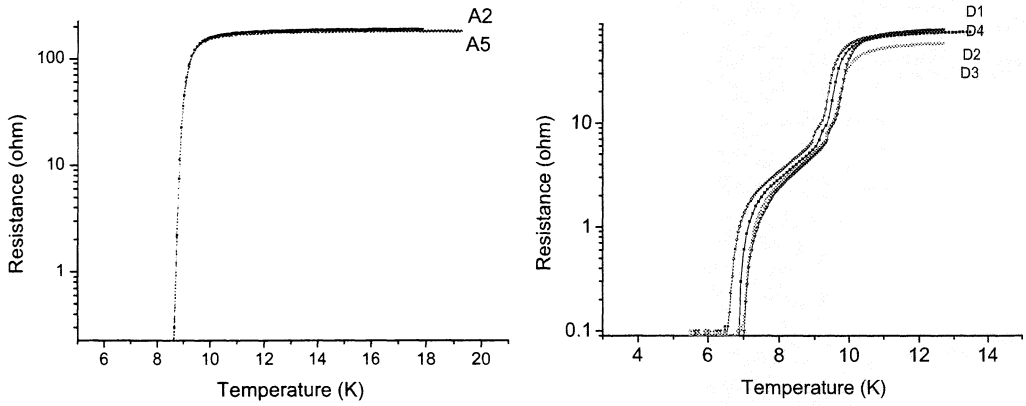

Figure 4: Resisatnce versus temperature curves of type A (left) and type D (right) devices. (All devices have similar lengths, except for device D3, which is shorter). Note that T_{c2} (lower value) is identical for devices with the same contact. This indicates good process control of the interface.

For devices of type A we only observe one transition temperature, indicating that the critical temperature of the pads is identical to the one of the bolometer. This is consistent with our understanding that there is a contact resistance in between the layers.

Fig. 5 shows R(T) curves measured for several devices with an intermediate superconducting layer contact, which might suppress the reduction of T_c of the pads by the proximity-effect (with Nb, type H (left), and with NbTiN, type G (right)). These devices show normal state resistance values ranging from 56 to 78 Ω, depending on bridge length. In addition the overall shape of the resistive transition is quite comparable to those of type D devices.

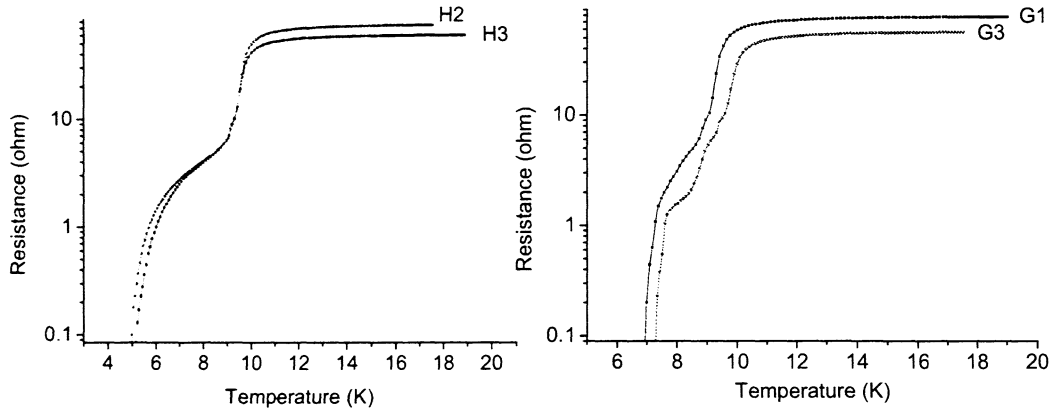

Fig.5 R(T) curves of devices with superconducting intermediate layers (type H with Nb (left) and type G with NbTiN (right)). H3 and G3 are shorter. *Note that the T_{c2} values are identical for the devices with same contact types.*

All data have been summarized in Table 1. A small difference remains between measured resistance values and calculated ones (between brackets). Whether this is due an uncertainty in the value for the sheet resistance or reflects a remnant contact resistance is not known. Note that devices of type D, G and H have similar T_{c1}'s (9.9 K) but different values of T_{c2}. The latter value is interpreted as reflecting the critical temperature of the contact pads.

Table 1, Summary of measured DC parameters of devices of batch M2S. containing devices with four different types of contacts. R_{11K} and $R_{300\,K}$ are the resistance measured at 11K and at the room temperature. The expected values for R_{11K} are estimated from the bridge size and the sheet resistance of the NbN film . RRR is the ratio between $R_{300\,K}$ / R_{11K}. T_{c1} is the critical temperature of the bridge and T_{c2} the contact pads. determined from the RT curve. I_{c1} is the maximum critical current measured manually in the current-bias mode.

Device	R_{11K} (expected)	$R_{300\,K}$	RRR	T_{c1}	T_{c2}	I_{c1}
A1	147 Ω	98 Ω	0.67	*	9.5 K	311 mA
A3 Only O_2 Etch	218 Ω	116 Ω	0.53	*	9.3 K	345 mA
A4	236 Ω	135 Ω	0.59	*	9.3 K	348 mA
D1	79 Ω	67 Ω	0.83	9.7 K	6.7 K	367 mA
D2 O_2 + Ar Etch	86 Ω	70 Ω	0.83	9.8 K	7.0 K	451 mA
D3	59(52) Ω	53 Ω	0.91	9.9 K	7.1 K	478 mA
D4	80 Ω	72 Ω	0.91	9.9 K	7.1 K	499 mA
H2 In Situ	78(60) Ω	65 Ω	0.83	9.8 K	5.3 K	436 mA
H3 Nb	62(52) Ω	53 Ω	0.83	9.7 K	5.3 K	400 mA
G1 In situ	78 Ω	65 Ω	0.83	9.5 K	7.0 K	456 mA
G3 NbTiN	56(52) Ω	50 Ω	0.91	9.9 K	7.2 K	515 mA

4. Transition Temperatures of Bi-layers

For a quantitative understanding of the possible T_c variations in stacks of contact layers we study a few typical bilayers using the proximity-effect model developed by Golubov et al. [9]. The model contains the intrinsic T_c's, the resistivities and the thicknesses of the different layers as well as the interface transparency. Even for a chemically clean interface the transmissivity will still differ from unity because of Fermi velocity mismatch. Fig. 6 shows the reduced transition temperatures t (T/T_c) for three different cases: NbN (3.5 nm)/Au (70 nm), Nb (5 nm)/Au (45 nm), and NbTiN (10 nm)/Au (40 nm), as a function of interface transparency.

For NbN/Au the reduction of T_c has a strong dependence on the transparency, because the NbN is extremely thin. A transparency of 0.05 is already enough to push the T_c to below 4 K (T_c =9.9 K for NbN). Since type A devices show a minor reduction in T_c, the interface transparency must be smaller than 0.005. For type D devices we find experimentally a reduced temperature of 0.7-0.8, which would be consistent with a transparency between 0.01-0.02. This value is considerably smaller than the value of ~0.2, which we expect form the Fermi velocity mismatch based on $v_f = 1.39 \times 10^6$ m/s for Au [16] and $v_f = 5.7 \times 10^4$ m/s for a NbN film [17].

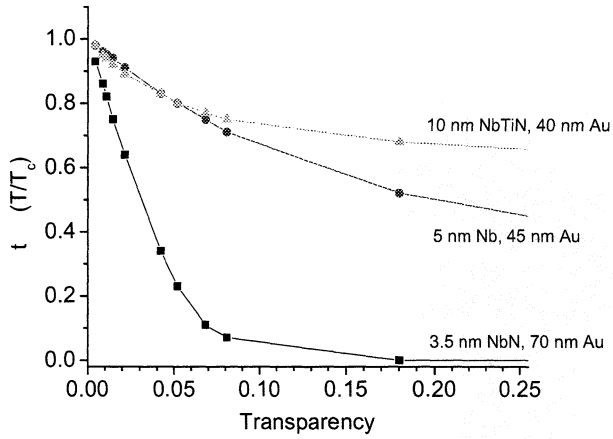

Fig. 6. Reduced critical temperature (T/ T_c) as a function of interface transparency calculated for three different bilayers, NbN/Au, Nb/Au and NbTiN/Au.

We also use the results of Fig.6 to determine an expected value for the T_c of the bilayers involved. For the Nb/Au interface we assume a transparency of 0.5, which is calculated using $v_f = 2.77\times10^5$ m/s for Nb [18]. Using a T_c of 6 K for the Nb film, we expect a T_c for the contact bilayer of 1.8 K. For temperatures far above 1.8 K, we can treat this contact layer as a single normal metal layer. Unfortunately we have no data for the Fermi-velocity of NbTiN film. To proceed we assume the transparency of the NbTiN/Au interface to be the same as for Nb N/Au (~0.2). Using this we find an expected T_c of the NbTiN/Au layer of ~ 5-6 K, using a T_c of 8 K for the NbTiN film.

Type H contacts show a T_{c2} of 5 K, i.e. a reduced critical temperature of 0.5-0.6. Assuming that we can indeed treat the Nb/Au bilayer as a fully normal layer, more specifically as a single Au layer we can apply the calculated curve for NbN/Au of Fig. 6. From this we find a relatively small interface transparency of 0.02-0.03 in Type H devices between NbN and the contact layer.

Type G devices have an identical interface between the NbN and the intermediate layer because the interface was made in the same way. If we use the transparency value of Type H contact for Type G as well we find a consistent value for T_{c2} (7.1 K).

We conclude by emphasizing that the transparency for Type H and G contacts is still relatively low, T~0.02-0.03, compared to the expected maximum value of T=0.2. However, it is better than for Type D (T~0.01-0.02), probably because of the in-situ deposition. It certainly indicates that the deviation between the expected and measured resistances as listed in Table 1 may be partly due to the interface resistance.

5. Current versus Voltage measurements

The R(T) measurements and the evaluation of the proximity-effect model build a coherent picture, suggesting that the successful device-types G and H consist of NS'SS'N devices with N representing the Au antenna wiring, S' the contact pads and S the active superconducting layer. S' has a slightly lower T_c than S if measured with a low bias current. In actual use HEB's are cooled down to a bath temperature of 4.2 K or lower, and then biased by a DC voltage, which establishes a working point for the mixer by the formation of the electronic hot spot. The evolution towards this working point can in principle be followed in the current-voltage characteristics. In interpreting the I,V curves one extra element has to be kept in mind. The variation in thickness (or cross-section) causes the local current density to be highest in the active NbN material. And a variation in current-density might cause a variation in local power-density when normal. However, the variation in thickness as well as the nature of the materials should also be dealt with in establishing the heat out-flow conditions. Therefore I,V curves are not easily interpretable.

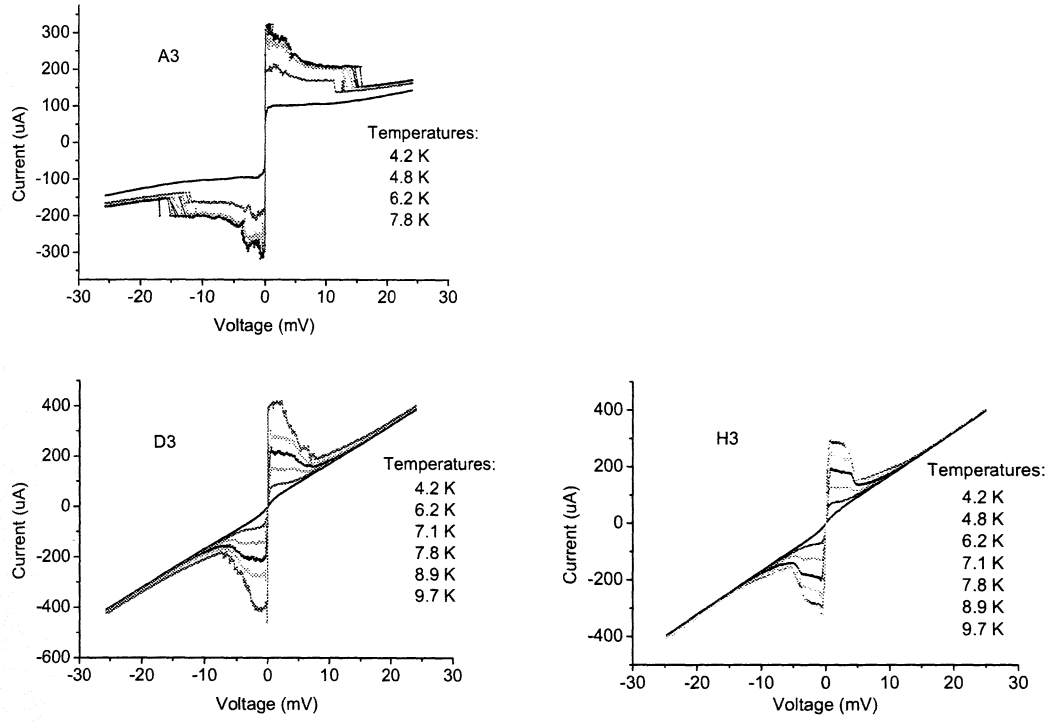

Figure 7, IV curves of devices with contact type A, D and H, measured at different temperatures. The curve for type G is not shown since at this voltage range it is very similar to the curve of type H.

Fig. 7 shows I,V curves of typical devices of type A, D, and H, measured using a voltage bias for various bath temperatures from 4.2 K to about 10 K. For Type A devices a rather broad feature is visible at low voltages ending around ±15 mV. Beyond 15 mV, the IV curves do not overlap for different temperatures. Similar features have been reported for devices fabricated in similar way [2,3]. As argued before these devices have a rather large contribution to the resistance due to the NbN/Au interface, which will contribute as local source of dissipation, which will influence the formation of a usable hot spot. Since this broad feature appears only

for type A devices we believe that this contact resistance plays a role. Note that it appears directly after the critical current is exceeded at the lowest voltages. It is know that in this regime a negative resistance region appears causing time-dependent relaxation–oscillations. So the actual shape might be a time-averaged result and not necessarily informative about the DC I,V curve.

I,V curves of type D and H contacts do not show these broad shoulder-like structures. Instead we observe a much narrower features at low voltages followed by a smooth transitions of the IV curves to a regime with positive resistance This transition takes place within a bias voltage ± 10 mV for type D and ± 5 mV for type H. The change of IV curves from low temperatures to T_c behaves very similar to what one expects from the electronic hotspot model [12,13]. All the IV curves at high bias overlap for different bath temperatures, indicating that a normal resistive hot spot is established and that the resistance of the contact pads does not play a role.

The dissipative state characteristic of a fully established hot spot is reached by starting with a nearly zero-resistance state. For increased current a critical value is reached after which the normal state is approached through some intermediate state. Therefore, we also checked the critical current of various types of devices at 4.2 K. The results are also included in Table 1. These reported values are measured manually using the current-bias mode. Slightly lower values are found from the I,V curves recorded in the voltage-bias mode. For Type A devices the maximum critical current, defined as I_{c1}, varies substantially. However, it is clear that Type A devices have the lowest critical current, while the type G devices the highest value.

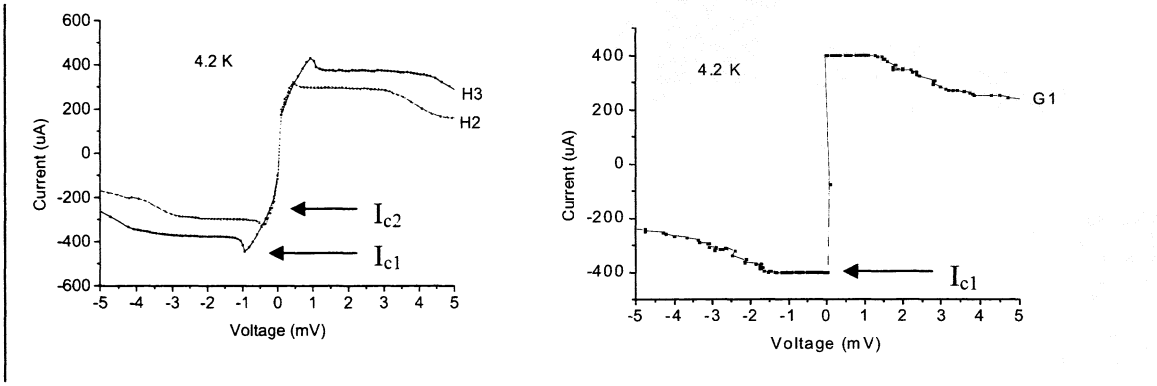

Figure 8. On the left side: the IV plots of device type H; on the right side, the IV plots of type G. All curves are taken around the zero bias voltage and at 4.2 K.

In Fig. 8 the I,V curves for Type H and G devices are shown on an expanded voltage scale. In Type H devices (Nb intermediate layer) we observe at low voltages two critical currents. The slope of the IV curve above the kink corresponds to a dynamic resistance of ~ 3.5 Ω. I_{c1} is defined as the highest critical current where the voltage rapidly increases and the hot spot is formed. The lower critical current I_{c2} signals the onset of a resistive state with a value much lower than can be attributed to a fraction of the bridge being normal. It is reminiscent of features observed in superconducting microbridges and might also reflect flux-flow or phase-slip behaviour. This lower critical current, I_{c2}, decreases with increasing temperature and disappears completely when the temperature reaches T_{c2} for the pads. We therefore believe that I_{c2} is related to the contact pads, which implies that the small dynamic resistance signals

the resistance associated with the conversion of the currents from N' (S' in the normal state) and S the active superconducting layer.

These two critical currents are strikingly absent in devices of Type G (NbTiN intermediate layer). This suggests that the I_{c2} associated with the pads is either equal to or larger than I_{c1}. Such a difference might qualitatively be understood by the differences in T_c. However, the important issue is what conditions are established for the electronic hot spot when operated as a mixer. These remain to be worked out.

6. Conclusions

The crucial importance of the contacts between the Au antenna and the active NbN layer in phonon-cooled hot-electron bolometers has been demonstrated. Best results have been obtained with contacts in which a NbTiN layer is inserted between the Au and the NbN. Devices *without* physical cleaning of the NbN surface have significant contact resistance ($\sim 100\ \Omega$). Devices with contact pads *with* physical cleaning of the interface show negligible contact resistances ($<10\ \Omega$). It is argued that the interface transparencies are still not close to unity (0.01-0.02 for ex-situ and slightly better (0.02-0.03) for in-situ deposited contact pads). The results suggest that further optimisation of mixer performance is to be found in improving further the transparency and determining the optimal use of the superconducting intermediate layer.

Acknowledgement: We would like to thank Z. Wang and S. Miki from Communication Research Laboratory in Japan for providing high quality thin NbN films, which were used for the development of the process. We are grateful for stimulating discussions with M. Kroug and T. Zijstra at Delft, P. Khosropanah and H. Merkel at Chalmers. This work is supported partly by the European Space Agency (ESA) under Contract No. 11653/95/NL/PB

Corresponding author: *m.hajenius@tnw.tudelft.nl*

References:

1. J. Kawamura, R. Blundell, C-y E. Tong, G. Gol'tsman, E. Gershenzon, B. Voronov, and S. Cherednichenko, *"Low noise NbN lattice-cooled superconducting hot-electron bolometric mixers at submillimeter wavelengths"* Appl. Phys. Lett. **70**, 1619 (1997)
2. P. Yagoubov, M. Kroug, H. Merkel, E. Kollberg, G. Gol'tsman, S. Svechnikov, E. Gershenzon, *"Noise temperature and local oscillator power requirement of NbN phonon-cooled hot electron bolometric mixers at terahertz frequencies"*. Appl. Phys. Lett. **73**, 2814 (1998).
3. A.D. Semenov, H.-W. Hübers, J. Schubert, G.N. Gol'tsman, A.I. Elantiev, B.M. Voronov, E.M. Gershenzon, *"Design and Performance of the Lattice-Cooled Hot-Electron Terahertz Mixer"*, J. Appl. Phys. **88**, 6758, (2000).
4. S. Miki, Y. Uzawa, A. Kawakami, Z. Wang, "IF Bandwidth and Noise Temperature Measurements of NbN HEB Mixers on MgO Substrates", *IEEE Trans. On Appl. Supercon.* **11 (1)**, 175, 2001.
5. T. Lehnert, H. Rothermel, and K. H. Gundlach, *"Low-noise heterodyne mixing with NbN microbolometers at 800 GHz"*, J. Appl. Phys. 83, 3892 (1998).
6. E. Gerecht, C.F. Musante, Y. Zhuang, M. Ji, K.S. Yngvesson, T. Goyette, and J. Waldman, Proc. 11th Int. Symposium Space THz Technolg, May 1-3, 2000, Ann Arbor, Michigan, pp 209
7. http://astro.estec.esa.nl/SA-general/Projects/First/first.html

8. J.J.A. Baselmans, M. Hajenius, J.R. Gao, T.M. Klapwijk, P.A.J. de Korte, B. Voronov, G. Gol'tsman. "Noise Performance of NbN Hot Electron Bolometer mixers at 2.5 THz and its dependence on the contact resistance", *Proc. of 14th Int. Symp. Space THz Technology*, Tucson. USA, March 2003. We note that the noise temperature of 1000 K is determined using the Callen and Welton definition.
9. A.A. Golubov, "Proximity effect in dirty N/S multilayers", Superconducting Superlattices and Microstructures, I. Bozovic, ed., SPIE proc. 215 (SPIE, Bellingham, WA, 1994), p353; A.A. Golubov, E.P. Houwman, J.G. Gijsbertsen, V.M. Krasnov, J. Flokstra, H. Rogalla, and M. Yu. Kupriyanov, Phys. Rev. B51, 1073 (1995).
10. M. Kroug, "NbN Hot Electron Bolometric Mixers for a Quasi-Optical THz Receiver", *Ph.D. Thesis*, Chalmers University, 2001, also P. Yagoubov, M. Kroug, H. Merkel, E. Kollberg, J. Schubert and H-W. Hübers, "*NbN hot electron bolometric mixers at frequencies between 0.7 and 3.1 THz*" , Supercond. Sci. Technol. **12**, 989-991, 1999.
11. J.H. Greiner, "*Josephson Tunneling Barriers by rf Sputter Etching in an Oxygen Plasma*", *J. Appl. Phys.* **42**, 5151, 1971.
12. D. Wilms Floet, E. Miedema, T.M. Klapwijk, and J.R. Gao, "*Hotspot Mixing: a Framework for Heterodyne Mixing in Superconducting Hot Electron Bolometers",* Appl .Phys. Lett. 74, 433 (1999).
13. H. Merkel, P. Khosropanah, P. Yagoubov, and E. Kollberg, Proceedings Tenth International Symposium Space Terahertz Technology, University of Virginia, Charlottesville, March 16-18, 1999. p. 592.
14. D. Wilms Floet, J.J.A. Baselmans, T.M. Klapwijk, and J.R. Gao, *"Resistive transition of niobium superconducting hot-electron bolometer mixers"*, Appl. Phys. Lett. 73, 2826 (1998).
15. A.H. Verbruggen, T.M. Klapwijk, W. Belzig, and J.R. Gao, "*The resistive transition of aluminium hot electron bolometer mixers with normal metal cooling banks*", *Proc. of 12th Int. Symp. Space THz Technology*, San Diego, USA, Page 42, February 2001.
16. N.W. Ashcroft and N. David Mermin, Solid Sate Physics, W.B. Saunders Company, International Edition, Philydelphia (1976)
17. Derived from measured coherence length ξ_0 in NbN film: A.D. Semenov, G.N. Gol'tsman, A.A. Korneev, "Quantum detection by current carrying superconducting film", Physica C, (351), pp. 349-356, 2001
18. H.R. Kerchner, D.K. Christen, S.T. Sekula, "Critical fields Hc and Hc2 of superconducting niobium" Phys. Rev. B 24 ,1200, 1981.
19. M. Hajenius, "The DC Characterisation of a superconducting HEB using a Niobium-Gold bilayer", *Grad. Report TU Delft*, April 2002.